PROCEEDINGS OF SCIENCE

Pacific Ocean Neutrino Experiment: Expected performance of the first cluster of strings

F. Henningsen[a,*] **for the P-ONE Collaboration**

[a] *Simon Fraser University*
8888 University Drive, V5A 1S6 Burnaby, BC, Canada

E-mail: felix_henningsen@sfu.ca

The Pacific Ocean Neutrino Experiment (P-ONE) is a proposed large-volume neutrino telescope in the Northeast Pacific Ocean, off the coast of Vancouver Island, Canada. With more than one cubic-kilometer of instrumented deep sea volume, P-ONE will target measuring high-energy neutrinos to shed light on the nature of astrophysical accelerators and the cosmos. With low expected scattering in the deep ocean, water-based detectors theoretically allow for sub-degree event resolution but carry various challenges. With changing ocean currents, and an abundance of organic matter, the detector geometry, water optical properties, and bioluminescent light background vary with time. This dynamic environment of the deep ocean requires rugged detector technologies and multiple, precise calibration and monitoring systems in order to enable and maintain the detector's full scientific potential. In cooperation with Ocean Networks Canada (ONC), the P-ONE collaboration aims to develop long-lived, deep-sea detector systems which target continuous and precise monitoring to overcome these challenges. The first mooring of P-ONE will be deployed between 2024 and 2025, and will provide first insights into the performance of the developed detector systems. Following this first step, this work summarizes the ongoing efforts of the P-ONE collaboration targeting the development, simulation and operation of the first cluster of strings, and will present the expected performance of the calibration systems and physics potential.

38th International Cosmic Ray Conference (ICRC2023)
26 July - 3 August, 2023
Nagoya, Japan

*Speaker

PoS(ICRC2023)1053

1. The Pacific Ocean Neutrino Experiment

The Pacific Ocean Neutrino Experiment (P-ONE) [1] aims to build a cubic-kilometer neutrino detector in the North-East Pacific Ocean, and will measure atmospheric and astrophysical neutrinos at high energies via secondary photons created by neutrino interactions. These measurements can be used to localize and study high-energy neutrino sources within the Universe. Identification of these sources is primarily driven by the number of neutrino observations and their directional reconstruction precision. Thus, extended coverage of the neutrino sky is necessary to increase the detection rate of neutrinos, advance the study of their sources, and uncover the unknown astrophysical phenomena associated with the highest-energy particle accelerators in the Universe. Additionally, water-based experiments can theoretically reach angular resolutions close to the kinematic limit of deep-inelastic neutrino interactions due to an effective scattering length in water of order 100 m. This will further ease particle identification within detected events. When completed, P-ONE will provide complementary sky coverage to IceCube [2] and the ongoing effort of the KM3NeT experiment in the Mediterranean Sea [3], advancing the global network of neutrino astronomy.

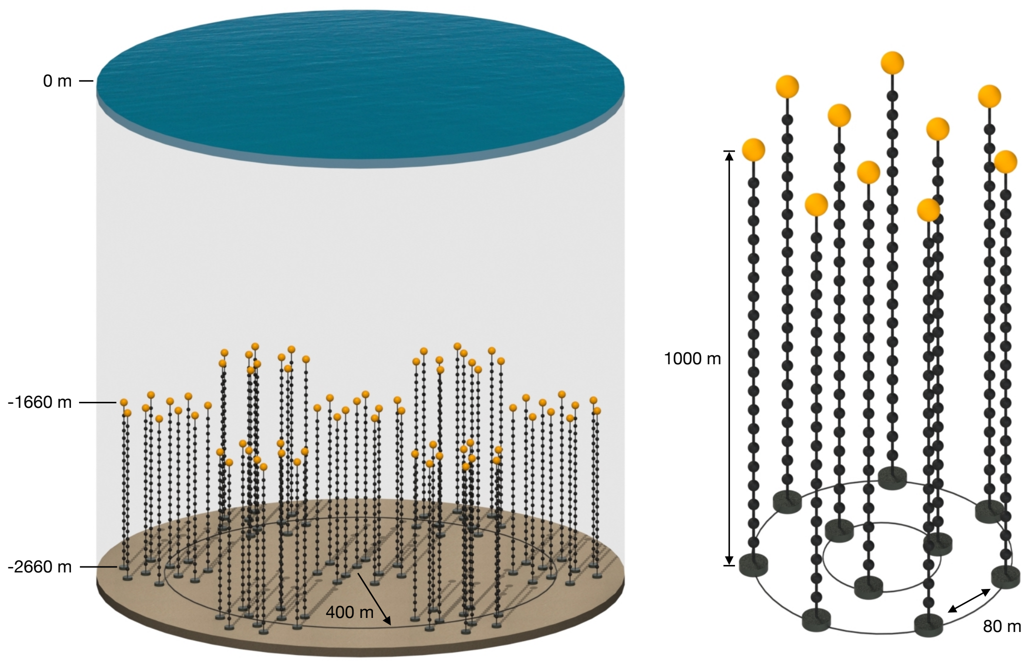

Figure 1: Pacific Ocean Neutrino Experiment vision. The pictures show the full P-ONE detector comprised of seven clusters with ten instrumented mooring lines each (left) and a more detailed view of a single cluster, i.e. the P-ONE demonstrator (right). Figure adapted from Ref. [1].

Figure 1 shows the P-ONE detector as envisioned in the Cascadia Basin abyssal plane at a water depth of 2660 meters, which is located off the coast of Vancouver Island, Canada. In collaboration with Ocean Networks Canada (ONC), P-ONE will leverage both the NEPTUNE deep-sea fiber-optic cable network to provide power and optical communication to the detector, and the ONC sea operations expertise to design and deploy a rugged detector design with a target lifetime of 25 years. The site has been thoroughly investigated with two pathfinder missions: Strings for

Absorption length in Water (STRAW) [4] and STRAW-b [5], installed with ONC at the Cascadia Basin site in 2018 and 2020, respectively. These missions verified the suitable optical properties and backgrounds of the Cascadia Basin deep sea [6, 7], as well as the reliability of ONC operations. The vision for P-ONE is to install more than 70 instrumented mooring lines (or *strings*) each 1 km in length. The strings will be equipped with 20 optical detection modules each, which are evenly spread along the entire length of the mooring. It is further envisioned that they are deployed in groups or clusters, providing a segmented geometry. In combination with low scattering in the deep-sea water of the Pacific Ocean, this will allow exceptional directional reconstruction of neutrino events, especially horizontal tracks. Furthermore, it will reduce the risk and complexity of necessary deep-sea operations. The P-ONE demonstrator is defined as the first cluster of the P-ONE detector, comprised of ten instrumented mooring lines, and connected to the ONC deep sea network. The development of the first P-ONE prototype line [8] is ongoing with a planned deployment between 2024/25, and future lines to follow thereafter.

2. P-ONE detector instrumentation

The P-ONE prototype line consists of 20 instruments spread evenly along its full length of 1 km and connected by a hybrid fiber-optic/copper cable. Along the mooring line, detection and calibration modules carry photomultiplier tubes (PMTs) and calibration systems. A mooring junction box (mJB) terminates the string and connects it to the ONC network infrastructure. The main target of the P-ONE prototype line and the demonstrator is to test the system components and deployment strategy within the deep sea environment, and to verify the expected detector performance. For more technical details refer to Ref. [8].

2.1 Detector infrastructure

The P-ONE hybrid fiber-optic/copper cable is a single, deep sea-applicable cable that carries fiber communication and power to each of the instruments along its full length of 1 kilometer. These connections to individual modules are realized using a segmented cable. Here, the required fiber and copper connections are spliced iteratively from the main cable at each instrument termination frame. This novel termination process allows using a single cable for the whole string while maintaining the possibility to exchange full cable segments. The termination frames are made from titanium and their splicing and sealing mechanisms assure cable integrity even in the case of individual module failures. On the surface end, the mooring line terminates with a buoyancy that maintains the upright position of the string. On the seafloor end, the cable terminates in the mJB which hosts power controllers for each instrument, a synchronization unit, and a connection to the NEPTUNE network node. Here, a rugged steel tray is used to mount the mJB and to act as both a deployment tray and an anchor. Prior to deployment, the string is coiled up on the tray, lowered to the sea floor, and unfurled once the anchor is in place. Data acquisition (DAQ) synchronization of the P-ONE detector is achieved using the BlackCat system. This custom development employs the concept of the White Rabbit (WR) protocol [9] but without using WR switches. Instead, a syntonous operation on layer-1 of Gigabit Ethernet (GbE) ensures sub-nanosecond synchronization between a central clock and all receiver endpoints. More details on the prototype line and synchronization systems are presented in Refs. [8] and [10], respectively.

2.2 Optical modules

The two main types of instruments located on the P-ONE mooring lines are shown in Figure 2. They can be categorized into regular optical modules (P-OMs) and calibration modules (P-CALs). Both are encapsulated in 17 inch borosilicate glass hemispheres, are equipped with PMTs for light detection, and are attached to the same instrument termination frame on the mooring line. However, while the P-OM carries eight PMTs per hemisphere, the P-CAL replaces four of them with different calibration systems – see section 2.3. In total, 20 modules are located on each string, with up to 3 of them being P-CALs, and the remainder P-OMs. Optical coupling of the PMTs to the glass hemispheres is achieved using custom gel pads that are molded to the photosensitive area prior to assembly within the glass hemispheres. A custom, high-voltage sub-system [11] provides each PMT with a self-regulated, programmable high-voltage supply. Analog output signals of the PMTs are fed to the P-OM mainboard where they are digitized with an ADC at a rate of around 200 MHz. A field-programmable gate array (FPGA) provides the mainboard with a central control logic operating a Linux operating system and controlling DAQ, peripheral devices, synchronization, and communication. Each module is equipped with several temperature, pressure, humidity, acceleration, and magnetic field sensors for continuous system monitoring.

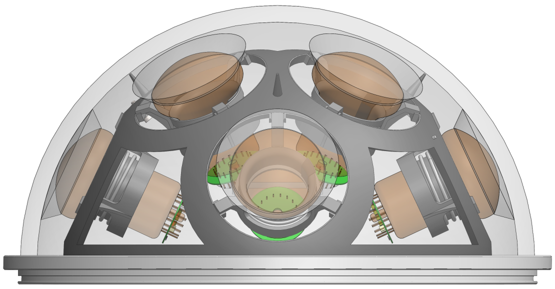

(a) P-ONE optical module – P-OM.

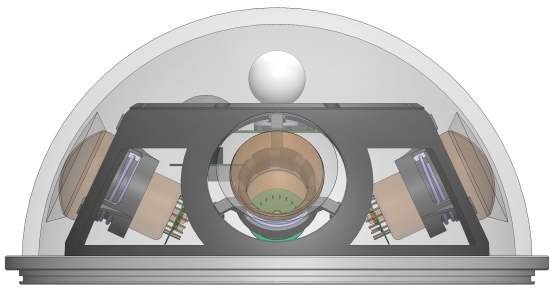

(b) P-ONE calibration module – P-CAL.

Figure 2: **(a)** P-ONE optical module and **(b)** calibration module. Each is equipped with PMTs, frame and calibration systems. More details on both instruments can be found in Refs. [8] and [12], respectively.

2.3 Calibration system

Real-time monitoring and calibration are of major importance for ocean-based detectors due to the dynamic deep sea environments. The detector geometry, water optical properties, and bioluminescent light backgrounds vary with time due to changing ocean currents. Thus, the P-ONE calibration system, shown in Figure 3, comprises three main concepts: beamed and isotropic optical light pulsers, an acoustic positioning system, and integrated devices to measure sedimentation, acceleration, magnetic fields, and environmental parameters. In combination with the PMTs, these systems allow continuous monitoring of calibration parameters. Ten beamed, sub-nanosecond light flashers are integrated into every module, targeting measurements of time synchronization between instruments, light scattering, and spectral dispersion. P-CALs are further equipped with isotropic, high-power, nanosecond light pulsers, and a self-monitoring system [12] based on the Precision Optical Calibration Module (POCAM) [13]. This system determines the calibration of optical water properties, module efficiencies, and sedimentation. The acoustic positioning system is comprised of an acoustic transceiver system on the sea floor and acoustic receivers [14] in each instrument. This allows precise monitoring of the string and module positions. At a later stage, acoustic positioning is planned to verify the introduction of a potential optical positioning system. Using sub-nanosecond light pulsers, a continuous, optical geometry calibration of P-ONE is envisioned. Lastly, in addition to environmental sensors included in all modules, P-CALs are further equipped with a camera system for monitoring sedimentation, biofouling, and bioluminescence.

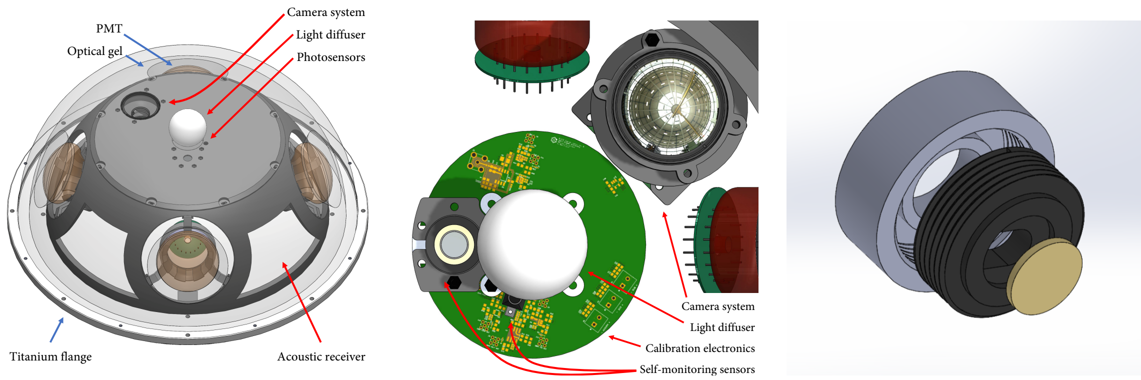

(a) P-CAL hemisphere layout **(b)** P-CAL calibration systems. **(c)** Acoustic receiver prototype.

Figure 3: P-CAL layout and calibration systems. **(a)** P-CAL hemisphere layout **(b)** P-CAL internal optics, self-monitoring and camera system and **(c)** the acoustic receiver which is installed in every module. More details on these systems can be found in Refs. [12] and [14], respectively.

3. First performance studies

We present the first results of simulation studies for the P-ONE demonstrator. This detector consists of a cluster of ten P-ONE mooring lines assuming a line spacing of 80 meters, a total line length of one kilometer, and 20 optical modules with a subsequent inter-module spacing of 50 meters. The radioactive background produced by Potassium-40 (K-40) on STRAW and P-ONE optical modules is estimated using a GEANT4 [15] simulation framework. The coincidence rate between PMTs in the P-OM, equipped with 16 PMTs, was studied based on experimental background data measurements taken with STRAW. Figure 4 shows the results of this study with low expected rates of high-level coincidences when compared to atmospheric muon background. These pathfinder measurements and follow-up studies on P-ONE performance characteristics allowed us to gain a detailed understanding of in-situ backgrounds. Precise calibration of the instrument positions in swaying ocean currents is of primary importance to reach the anticipated pointing precision. An acoustic multilateration study was done using the expected speed

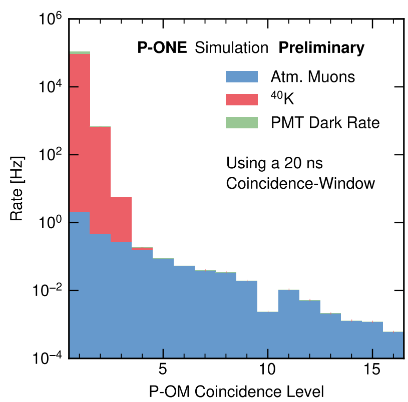

Figure 4: K-40 background simulation showing coincidence level rates between PMTs in the P-OM.

of sound profile in seawater [16], and three acoustic beacons around the cluster in a circle of 250 meters radius. The P-ONE study shown in Figure 5 is using a Markov-chain Monte Carlo (MCMC) method to fit the geometry based on simulated data. Results of this indicate a precision of around 10 cm for the relative geometry fit. It employs a causally-connected line model and an initial positioning uncertainty of beacons and anchors of $\sigma_{\text{pos}} = 2$ m. The absolute longitude and latitude positions in the global reference frame are finally characterized to centimeter precision in collaboration with the Northern Cascadia Subduction Zone Observatory (NCSZO) project [17, 18]. A similar study using nanosecond light sources for optical geometry calibration results in relative fit precision of 25 cm prior to accounting for calibration parameters of photon propagation, especially dispersion, in the water column. This gives reason to believe that a purely optical geometry calibration can also be realized to a precision of below 10 cm. The verification of this will be one of the key calibration studies of the P-ONE demonstrator.

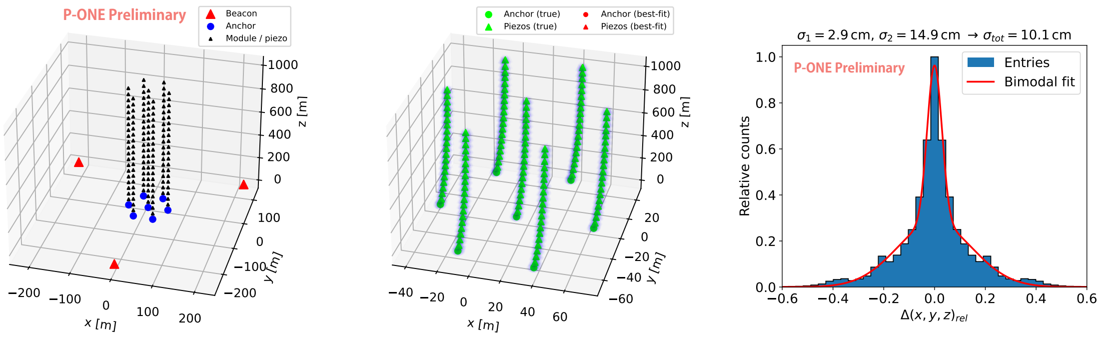

(a) MCMC study geometry baseline. **(b)** Example MCMC fit result. **(c)** Relative errors of the MCMC fit.

Figure 5: P-ONE demonstrator geometry calibration study using a bending model for the mooring line. **(a)** Study geometry baseline **(b)** An example MCMC fit result showing the true positions (circle), best-fit positions (triangle), and sampled region (shaded blue) **(c)** Positional errors of the example fit relative to the assumed truth showing a standard deviation of 10 cm. More details on this study can be found in Ref. [14].

The initial science studies of the P-ONE demonstrator use as a performance metric the characterization of its effective area, A_{eff}, and angular resolution, σ_{angular}. The effective area is a simulated, energy-dependent measure of the telescope's sensitivity to a neutrino flux. The angular resolution describes the precision of the reconstruction algorithm to reproduce the correct neutrino direction. Both parameters can be compared across different experiments, and depend on detector realization and optical properties of the medium. In its 70-string configuration, P-ONE combines an effective area at trigger level (minimum three PMTs hit in 10 ns) comparable to IceCube [19], with the excellent pointing resolution possible in ocean water. In-situ verification of this pointing will be possible with the P-ONE demonstrator using 10 strings. The study details presented in Ref. [20] for a 10-string (70-string) geometry confirm the excellent pointing resolution of neutrino tracks in water with a median angular resolution from 0.6 – 0.1 degrees (0.4 – 0.1 degrees)

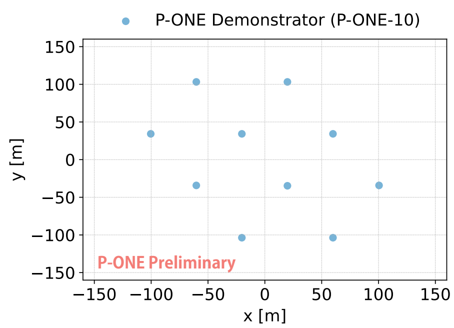

Figure 6: P-ONE demonstrator geometry.

at energies of 10 – 600 TeV. More details on detector optimization, and performance within the planetary neutrino monitoring system (PLENUM), are further given in Ref. [21].

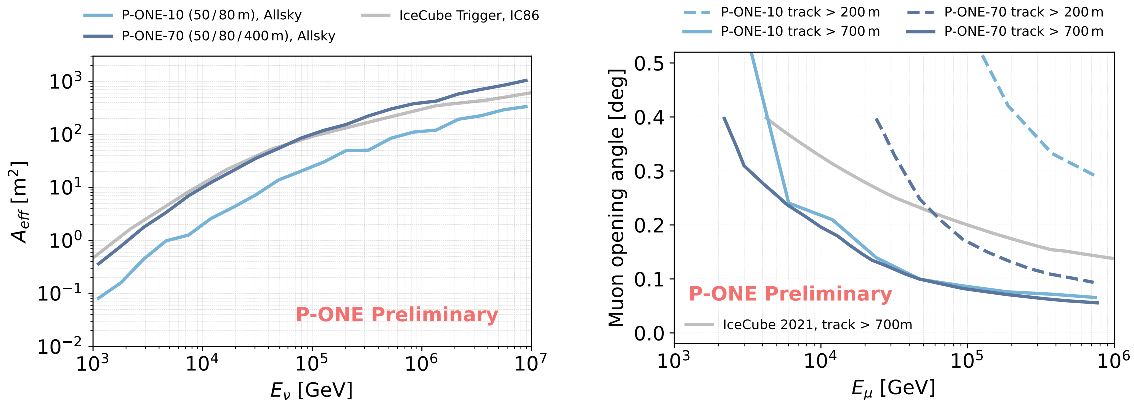

(a) P-ONE effective area. **(b)** P-ONE angular resolution.

Figure 7: P-ONE simulation results for both 10-string and 70-string geometries. **(a)** Effective area at trigger level (minimum three PMTs hit in 10 ns) as a function of neutrino energy in comparison to an IceCube reference [19] **(b)** P-ONE angular resolution as a function of muon energy shown together with an IceCube reference [22]. The study is based on simulated data for both 10- and 70-string geometries, and the labels indicate the used inter-module/line/cluster spacing. Both 10- and 70-string geometries assume 50/80 m module and line spacing, and the 70-string geometry additionally uses 400 m cluster spacing. Performance below ≈ 100 TeV is limited by the ability of the minimizer to locate the global minimum to the level shown here rather than the statistical limit at 1 TeV of 0.1 (0.2) degrees for 700 (200) m tracks. Improvement of minimizer convergence is a subject of ongoing work and more details on it can be found in Ref. [20].

The cosmic ray shadow caused by the moon is used to quantify, and verify, the expected excellent reconstruction performance of P-ONE (see Figure 7). A simulation study of the moon shadow was done to verify the expected performance of the P-ONE demonstrator using a simple trigger. This trigger only selected events that contained six or more optical modules that registered photons. Muons were simulated based on the expected atmospheric neutrino flux and live time of the detector and then shadowed according to the moon's position. The simulated event density is comparable to analyses by Icecube [23] and ANTARES [24], and a conservative analysis of the resulting angular distribution estimates the expected moon shadow after three years with a significance of at least 3.28 σ. Thus, this measurement provides a first promising case for verifying the anticipated pointing precision in situ.

4. Summary & outlook

The development of the P-ONE demonstrator is progressing rapidly, with the prototype line marking a significant milestone on the horizon. Scheduled for deployment in 2024/25, the P-ONE prototype line's timeline offers a valuable opportunity to gather extensive experience in deployment procedures, technical detector design, and the operation of the forthcoming P-ONE detector. The main goals of this phase comprise the verification of detector design and operations, the detailed understanding of in-situ calibration parameters, and the verification of the expected physics potential using first measurement of atmospheric muons and neutrino backgrounds.

Acknowledgements

We thank Ocean Networks Canada for the very successful operation of the NEPTUNE observatory, as well as the support staff from our institutions without whom P-ONE could not be operated efficiently. We acknowledge the support of Natural Sciences and Engineering Research Council, Canada Foundation for Innovation, Digital Research Alliance, and the Canada First Research Excellence Fund through the Arthur B. McDonald Canadian Astroparticle Physics Research Institute, Canada; European Research Council (ERC), European Union; Deutsche Forschungsgemeinschaft (DFG), Germany; National Science Centre, Poland; U.S. National Science Foundation-Physics Division, USA.

References

[1] M. Agostini et al., *Nature Astronomy* **2020**, *10*, 913–915.

[2] M. G. Aartsen et al., *JINST* **2017**, *12*, P03012.

[3] S. Adrian-Martinez et al., *J. Phys.* **2016**, *G43*, 084001.

[4] M. Boehmer et al., *JINST* **2019**, *14*, P02013.

[5] I. C. Rea et al. in *PoS ICRC2021*, *Vol. 395*, **2022**, p. 1092.

[6] N. Bailly et al., *Eur. Phys. J. C* **2021**, *81*, 1071.

[7] K. Holzapfel et al., P-ONE Collaboration in *PoS ICRC2023*, (these proceedings), **2023**.

[8] C. Spannfellner et al., P-ONE Collaboration in *PoS ICRC2023*, (these proceedings), **2023**.

[9] J. Serrano et al. in *Proceedings of ICALEPCS TUC004*, **2009**.

[10] M. Boehmer et al., P-ONE Collaboration in *PoS ICRC2023*, (these proceedings), **2023**.

[11] IceCube Collaboration in *PoS ICRC2021*, *Vol. 395*, **2022**, p. 1070.

[12] J. Stacho et al., P-ONE Collaboration in *PoS ICRC2023*, (these proceedings), **2023**.

[13] F. Henningsen et al., *JINST* **2020**, *15*, P07031–P07031.

[14] D. Ghuman et al., P-ONE Collaboration in *PoS ICRC2023*, (these proceedings), **2023**.

[15] S. Agostinelli et al., *Nucl. Instrum. Methods Phys. Res. A* **2003**, *506*, 250–303.

[16] P. G. Brewer et al., *Marine Chemistry* **2015**, *177*, 591–606.

[17] J. J. Farrugia et al. in OCEANS 2019 MTS/IEEE Seattle, **2019**, pp. 1–8.

[18] J. Hutchinson et al. in AGU Fall Meeting Abstracts, *Vol. 2022*, **2022**, G34A–04.

[19] A. Karle, IceCube Collaboration, IceCube, **2010**.

[20] J. P. Twagirayezu et al., P-ONE Collaboration in *PoS ICRC2023*, (these proceedings), **2023**.

[21] C. Haack et al., P-ONE Collaboration in *PoS ICRC2023*, (these proceedings), **2023**.

[22] R. Abbasi et al., *JINST* **2021**, *16*, P08034.

[23] IceCube Collaboration, *Physical Review D* **2014**, *89*, 102004.

[24] A. Albert et al., *Eur. Phys. J. C* **2018**, *78*, 1006.

Full Authors List: P-ONE Collaboration

Matteo Agostini[11], Nicolai Bailly[1], A.J. Baron[1], Jeannette Bedard[1], Chiara Bellenghi[2], Michael Böhmer[2], Cassandra Bosma[1], Dirk Brussow[1], Ken Clark[3], Beatrice Crudele[11], Matthias Danninger[4], Fabio De Leo[1], Nathan Deis[1], Tyce DeYoung[6], Martin Dinkel[2], Jeanne Garriz[6], Andreas Gärtner[5], Roman Gernhäuser[2], Dilraj Ghuman[4], Vincent Gousy-Leblanc[2], Darren Grant[6], Christian Haack[14], Robert Halliday[6], Patrick Hatch[3], Felix Henningsen[4], Kilian Holzapfel[2], Reyna Jenkyns[1], Tobias Kerscher[2], Shane Kerschtien[1], Konrad Kopański[15], Claudio Kopper[14], Carsten B. Krauss[5], Ian Kulin[1], Naoko Kurahashi[12], Paul C. W. Lai[11], Tim Lavallee[1], Klaus Leismüller[2], Sally Leys[8], Ruohan Li[2], Paweł Malecki[15], Thomas McElroy[5], Adam Maunder[5], Jan Michel[9], Santiago Miro Trejo[5], Caleb Miller[4], Nathan Molberg[5], Roger Moore[5], Hans Niederhausen[6], Wojciech Noga[15], Laszlo Papp[2], Nahee Park[3], Meghan Paulson[1], Benoît Pirenne[1], Tom Qiu[1], Elisa Resconi[2], Niklas Retza[2], Sergio Rico Agreda[1], Steven Robertson[5], Albert Ruskey[1], Lisa Schumacher[14], Stephen Sclafani[12α], Christian Spannfellner[2], Jakub Stacho[4], Ignacio Taboada[13], Andrii Terliuk[2], Matt Tradewell[1], Michael Traxler[10], Chun Fai Tung[13], Jean Pierre Twagirayezu[6], Braeden Veenstra[5], Seann Wagner[1], Christopher Weaver[6], Nathan Whitehorn[6], Kinwah Wu[11], Juan Pablo Yañez[5], Shiqi Yu[6], Yingsong Zheng[1]

[1]Ocean Networks Canada, University of Victoria, Victoria, British Columbia, Canada.
[2]Department of Physics, School of Natural Sciences, Technical University of Munich, Garching, Germany.
[3]Department of Physics, Engineering Physics and Astronomy, Queen's University, Kingston, Ontario, Canada.
[4]Department of Physics, Simon Fraser University, Burnaby, British Columbia, Canada.
[5]Department of Physics, University of Alberta, Edmonton, Alberta, Canada.
[6]Department of Physics and Astronomy, Michigan State University, East Lansing, MI, USA.
[8]Department of Biological Sciences, University of Alberta, Edmonton, Alberta, Canada.
[10]Gesellschaft für Schwerionenforschung, Darmstadt, Germany.
[11] Department of Physics and Astronomy and Mullard Space Science Laboratory, University College London, United Kingdom
[12] Department of Physics, Drexel University, 3141 Chestnut Street, Philadelphia, PA 19104, USA.
[13] School of Physics and Center for Relativistic Astrophysics, Georgia Institute of Technology, Atlanta, GA, USA.
[14] Erlangen Centre for Astroparticle Physics, Friedrich-Alexander-Universität Erlangen-Nürnberg, D-91058 Erlangen, Germany.
[15] H. Niewodniczański Institute of Nuclear Physics, Polish Academy of Sciences, Radzikowskiego 152, 31-342 Kraków, Poland.
[α] now at Department of Physics, University of Maryland, College Park, MD 20742, USA.